Preparation of nano α-Fe_2O_3 and γ-Fe_2O_3 and used for elemental mercury removal

Zengqiang Tan [1, *], Fanhai Kong [2]

[1] Huaneng Changjiang Environmental & Technology Co. Ltd., Beijing 100031, China
[2] Xi'an Thermal Power Research Institute Co. Ltd., Xi'an, Shannxi 710054, China

Abstract: The rod-shaped nano α-Fe_2O_3 and γ-Fe_2O_3 were prepared by a hydrothermal method. And the crystal phase structure, particle size, morphology and surface area of the synthesized nano α-Fe_2O_3 and γ-Fe_2O_3 were characterized by XRD and BET analysis. The removal of gaseous elemental mercury by nano α-Fe_2O_3 and γ-Fe_2O_3 was carried out on a fixed bed reactor. The effects of oxygen, bed temperature, particle size and acid flue gas components have been discussed. The results show that elemental mercury could be oxidized by nano α-Fe_2O_3 and γ-Fe_2O_3 with the presence of oxygen.

1. Introduction

The elemental mercury (Hg^0) emitted from coal combustion is a serious environmental problem, since its high toxicity and high volatility. Mercury released into the environment can be transformed into methyl-Hg, which could bio-accumulate in fish. The removal of Hg^0 is a key point for mercury removal [1].

The noble metals (such as gold and palladium) have good performance for the oxidation of Hg^0, but they are too expensive. The manganese oxides loaded on some carriers (e.g Al_2O_3) displayed significant oxidation capacity for Hg^0 at higher temperature [2]. The denitration device should be installed upstream of particulate control devices to obtain the optimum reaction temperature, which results in catalyst deactivation for exposure to fly ash. So developing catalysts operating at lower temperatures has been of great interest. For example, an adsorbent composed of active nano-layer on mesoporous silica substrate was developed by Abu-Daabes and Pinto [3], which was used to remove mercuric chloride under low-temperature (<135 ℃).

Particles can catalyze some reactions that are not feasible in particle-free systems [4]. Recently, the nano-sized metal oxides have attracted more attention for excellent catalytic decomposition performance of pollutants. Especially, the nano-sized metal oxides have densed surface unsaturated sites and smaller particle size, which could enhance catalytic capability of catalyst [5]. Among the nano-sized metal oxides, nano iron oxide has advantages of catalytic activity, toxicity resistance, and good performance in removal of carbon monoxide and sulfur dioxide [6].

The catalytic removal performance of Hg^0 by different crystal structure of iron oxide (α-Fe_2O_3 and γ-Fe_2O_3) has been controversial. Some studies concluded that γ-Fe_2O_3 is the main iron phase in ash, and γ-Fe_2O_3 played the dominant role in the catalytic removal of Hg^0 [7,8]. But Grant et al [9, 10] reported that the two crystalline structure of iron oxide had no significant removal effects for the Hg^0. Therefore, it is necessary to conduct detailed study of α-Fe_2O_3 and γ-Fe_2O_3 used for mercury removal. More importantly, the potential of the material in the nanoparticle form has not been explored.

In this study, α-Fe_2O_3 and γ-Fe_2O_3 nanoparticles were synthesized to remove Hg^0 and the mechanism was also studied.

2. Experimental

2.1 Synthesis of α-Fe_2O_3 and γ-Fe_2O_3 nanoparticles

The hydrothermal method was used to synthesize nano α-Fe_2O_3 catalyst. A starting material was $Fe(OH)_3$ prepared by adding a stoichiometric mixture of $FeCl_3 \cdot 6H_2O$ and NaOH. After vigorously stirred for 40 minutes at room temperature and pH of 12, the particle was separated and put into a high-pressure hydrothermal apparatus at 180℃ for 2 hour, the yellow product was centrifuged, rinsed with distilled water, and calcined at 500~600℃ for 4 hour. The obtained deep red α-Fe_2O_3 was collected for the following experiments and characterization. Polymer PEG was added to the reaction system as oxidant, surfactant and dispersing agent. The nano-α-Fe_2O_3 and PEG-400 were mixed and stirred fully for some time, then calcined at 400 ℃ to obtain pure crystalline γ-Fe_2O_3.

* Corresponding author: tanzq2008@126.com

2.2 Characterization of nanoparticles

The morphological observation of synthesized samples was conducted with a scanning electron microscope (Holand Quanta 200). The nitrogen adsorption apparatus (Micromeritics ASAP 2020) was used to determine the pore size distribution and Brunauer-Emmett-Teller (BET) surface area. The synthesized α-Fe_2O_3 and γ-Fe_2O_3 nanoparticles were investigated using X-ray powder diffraction (XRD) analysis (Holand) to understand the crystal phase structure. Using Scherrer equation, the crystal sizes of γ-Fe_2O_3 and α-Fe_2O_3 were calculated using formula (1).

$$D = \frac{K\lambda}{(\beta - \beta_1)\cos\theta} \quad (1)$$

Where, θ is diffraction angle, β_1 is half-intensity width from instrumental broadening, β is half-intensity width of the relevant diffraction peak, λ is X-ray wave length, K is half width, D is grain diameter.

2.3 Experimental method

The reactor consists of a quartz reactor insert tube (20 mm I.D.), the catalyst was put in the inner tube. The thickness of the sample bed was maintained around 3 mm. The simulated flue gas was N_2 stream containing O_2 (10%) and CO_2 (12%). The Hg^0 concentration was controlled by adjusting the water bath temperature and the N_2 flow rate passing through the mercury saturator. A "semi-continuous" mercury analyzer (VM3000, German) was used to monitor the Hg^0 concentration. 0.25 g of catalyst was used in each test, the flue gas rate was held at 2 L/min, the inlet Hg^0 concentration was 40 μg/m^3.

The Hg^0 removal performance is expressed by removal efficiency η according to formula (2). Wherein C_{outlet} and C_{inlet} represent the outlet and inlet Hg^0 concentration (μg/m^3).

$$\eta = (1 - C_{outlet} / C_{inlet}) \times 100\% \quad (2)$$

3. Results and discussion

3.1 Characterization

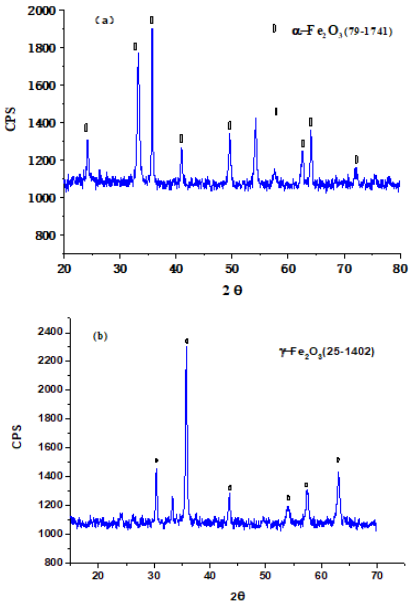

Fig. 1 X-Ray diffraction pattern of the synthesized nano-particle (a: α-Fe_2O_3 b: γ-Fe_2O_3).

The synthesized catalyst's XRD patterns of are shown in Fig.1. The narrow and high intensity peak at 33.142°and 35.654°could be observed from Fig.1(a). The single-phase formation of α-Fe_2O_3 structure could be confirmed corresponding to the JCPDS no. 174179. There are two obvious crystal phases around the peak at 2θ=36.5 and 2θ=63°(Fig.1(b)), which can be assigned to γ-Fe_2O_3 (JCPDS 25-1402). These above results suggested that the preparation of γ-Fe_2O_3 from α-Fe_2O_3 was successful.

Table 1. Properties of catalysts

Sample	BET Surface Area (m^2/g)	Total Pore Volume (cm^3/g)	Average pore size(nm)	Particle size (nm)
Nano α-Fe_2O_3	43.76	0.11	16.61	18.13
Nano γ-Fe_2O_3	36.54	0.09	15.12	27.24

Table 1 shows the properties of pure samples, the Fe_2O_3 nanoparticles with different size were prepared with different concentration of reactants and pH value. The BET surface area of samples was found to be in the range of 36.5~43.7 m^2/g, and pore size of nano samples was in the range of 15.1~16.6 nm.

3.2 Effect of reaction temperature

The reaction temperature plays an important role in the heterogeneous removal of Hg^0 by γ-Fe_2O_3 and α-Fe_2O_3 under O_2+N_2+CO_2 atmosphere (BL atmosphere). The effects of temperature on Hg^0 removal by nano Fe_2O_3 were evaluated in the range of 80-150℃.The oxidation

efficiency of Hg^0 by γ-Fe_2O_3 and α-Fe_2O_3 increased with the temperature increase as shown in Fig.2.

The enhancement performance of Hg^0 removal by γ-Fe_2O_3 and α-Fe_2O_3 with increasing temperature could attribute to the active sites increase for Hg^0 [11]. The chemical adsorption of Hg^0 could be enhanced by temperature increase. The surface functional groups and reaction temperature are significant in both adsorption and surface reactions.

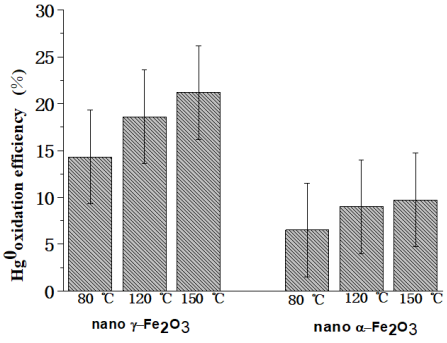

Fig.2 Hg^0 removal efficiency under different bed temperature.

Furthermore, the Hg^0 removal efficiency of γ-Fe_2O_3 is greater than α-Fe_2O_3 under the same operation conditions. The γ-Fe_2O_3 is spinel crystal structure with cation vacancy, the vacancies are distributed uniformly. But the α-Fe_2O_3 belongs to trigonal corundum-typed structure, and Fe^{3+} is surrounded by six equidistant oxygen. The metal-oxygen bond energy of α-Fe_2O_3 is -196.4 kcal/mol, smaller than that of γ-Fe_2O_3 (-191.7 kcal/mol). Moreover, the oxygen dissociation pressure of α-Fe_2O_3 is $10^{-13.8}$ torr, and that of γ-Fe_2O_3 is $10^{-8.8}$ torr. This implies that the oxygen of γ-Fe_2O_3 has higher thermodynamic chemical potential than that of the α-Fe_2O_3, companied with more favorable catalytic activity. This theory was confirmed by some researchers, who studied the catalytic reactivity of α-Fe_2O_3 and γ-Fe_2O_3 to butene, which showed that lattice oxygen of γ-Fe_2O_3 has higher activity than that of α-Fe_2O_3 [12,13].

3.3 Effect of oxygen

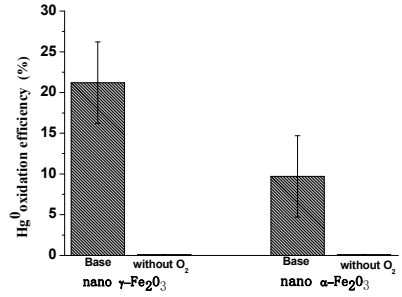

Fig.3 Hg^0 removal efficiency at 150℃ with different oxygen concentration.

To identify the influence of oxygen on Hg^0 removal, experiments were conducted with varied concentration of oxygen (0% and 6%) at 150℃. The Hg^0 removal efficiency was found to depend on oxygen (Fig.3). With the presence of 6% oxygen, the Hg^0 removal efficiency by γ-Fe_2O_3 and α-Fe_2O_3 increased from 0% to 21% and 10%, respectively. Li [5] found that CO could be oxidized by nano Fe_2O_3 through complicated route even without O_2. However, the experimental results proved that nano Fe_2O_3's Hg^0 removal ability was negligible without O_2. This observation is consistent with another study [14], and no obvious Hg^0 adsorption was observed when a gas stream of Hg^0/N_2 passed through the V_2O_5 catalyst.

The promotion effect of oxygen on Hg^0 removal could be explained by the Mars-Maessen mechanism [15]. The process of Hg^0 oxidation involves electron transfer. The adsorbed Hg^0 could react with lattice oxygen provided by the metallic oxides (M_xO_y), and the M_xO_y is Fe_2O_3, and the intermediate product M_xO_{y-1} could be Fe_3O_4 or FeO.

3.3 Effect of particle size

To study the effect of particle size on Hg^0 removal, the nano iron oxide catalyst and common iron oxide were tested under the BL atmosphere. The properties of iron oxide and mercury removal performance were summarized in Table 2. The common iron oxide is purchased iron oxide sieved with 200 mesh.

Table 2. The effect of property of iron oxide to mercury removal

	Nano α-Fe_2O_3-1	Nano α-Fe_2O_3-2	Common α-Fe_2O_3
BET surface area(m^2/g)	43.76	31.25	17.98
Total pore volume (cm^3/g)	0.11	0.091	0.02
Average pore width(nm)	16.61	14.86	6.10
XRD size (nm)	18.1	42.3	<7.0μm
Inlet concentration(μg/m^3)	40	40	40
90% breakthrough time(min)	45	35	<1

As can be seen from Table 2, the common α-Fe_2O_3 penetrated quickly under BL atmosphere, indicating that normal-sized α-Fe_2O_3 had almost no mercury removal ability. But the 90% breakthrough time of the nano α-Fe_2O_3 could last for more than 30 minutes. This observation implied that the unique catalytic property of nano α-Fe_2O_3 to the Hg^0. It possibly resulted from quantum size effect of nanomaterials and larger surface area, and larger surface area could provide more surface active sites for Hg^0 removal.

Fig.4 showed the Hg^0 removal efficiency by three catalysts with the presence HCl. The results were similar to that of BL atmosphere. The Hg^0 removal efficiency of ordinary-sized α-Fe_2O_3 was quite low, but the two nano-sized Fe_2O_3 showed a higher mercury removal efficiency. Furthermore, with the increased surface area and decreased particle size, the mercury removal efficiency had an increasing trend.

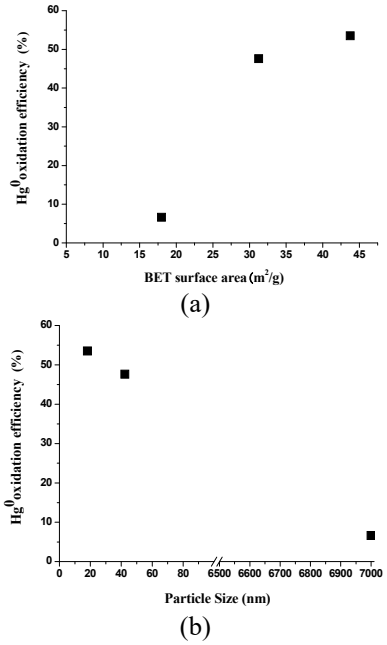

Fig.4 The effect of surface area(a) and particle size(b) to Hg^0 removal

4. Conclusions

In this study, the nano α-Fe_2O_3 and nano γ-Fe_2O_3 were synthesized successfully by hydrothermal method. The removal performance of Hg^0 by nano α-Fe_2O_3 and nano γ-Fe_2O_3 was studied with a fixed-bed reactor.

The normal-sized iron oxides had negligible mercury adsorption capacity under the BL atmosphere, but the nano α-Fe_2O_3 and nano γ-Fe_2O_3 showed obvious capacity for Hg^0. Furthermore, the nano γ-Fe_2O_3 showed greater oxidative capacity under the BL atmosphere. The increase of bed temperature and oxygen content were found to promote the mercury removal.

Acknowledgments

Project Supported by National Natural Science Foundation of China (51976072), Tsinghua-Huaneng Basic Energy Joint Research Institute (U20YYJC01), Scientific Research Project of Xi'an West Boiler Environmental Protection Engineering Co., Ltd. (GA-21-TZK01).

References

1. Ying Li, Liu YX, Yang W, Liu L, Pan JF. Adsorption of elemental mercury in flue gas using biomass porous carbons modified by microwave/hydrogen peroxide [J]. Fuel, 2021, 291, 120152.
2. Yao T, Duan Y, Zhu C. Investigation of mercury adsorption and cyclic mercury retention over MnOx/γ-Al_2O_3 sorbent [J]. Chemosphere, 2018, 202:358-365.
3. Abu-Daabes MA, Pinto NG. Synthesis and characterization of a nanostructured sorbent for the direct removal of mercury vapor from flue gases by chelation [J], Chem. Eng. Sci. 2005, 60, 1901–1910.
4. Hu J, Geng X, Duan Y. Effect of mechanical-chemical modification process on mercury removal of bromine modified fly ash [J]. Energy & Fuels, 2020, 34(8):9829-9839.
5. Li P, Donald E, Miser SR. The removal of carbon monoxide by iron oxide nanoparticles [J]. Appl. Catal. B: Environ. 2003, 43,151-162.
6. Reddy BV, Rasouli F, Hajaligol MR. Novel mechanism for removal of CO by Fe2O3 clusters. Fuel 2004, 83(11-12), 1537-1541.
7. Kurien U, Hu Z, Lee H. Radiation enhanced uptake of Hg0(g) on iron (oxyhydr) oxide nanoparticles[J]. Rsc Advances, 2017, 7(71):45010-45021.
8. Zhang Y, Mei D, Wang T, Wang J, Gu Y, Zhang Z, et al. In-Situ Capture of Mercury in Coal-Fired Power Plants Using High Surface Energy Fly Ash [J]. Environmental Science and Technology. 2019; 53(13):7913-20.
9. Grant ED, Raymond AD, Constance LS. Fixed- bed sdudies of the interactions between mercury and coal combustion fly ash [J]. Fuel Process Technol 2003, 82, 197-123.
10. Galbreath K C, Zygarlicke C J, Tibbetts J E. Effects of NOx, α-Fe_2O_3, γ-Fe_2O_3, and HCl on mercury transformations in a 7-kW coal combustion system [J]. Fuel Process Technol 2004, 86, 429-448.
11. Khedr MH, Abdel KS, Nasr MI. Effect of temperature on the catalytic oxidation of CO over nano-sized iron oxide [J]. Materials Science and Engineering A 2006, 430(1-2),40-45.
12. Antua-Nieto C, Rodríguez E, López-Antón M, García R, Martínez-Tarazona M. Carbon materials loaded with maghemite as regenerable sorbents for gaseous Hg0 removal [J]. Chemical Engineering Journal. 2020, 387:124151.
13. Trobajo J R , Antuna-Nieto C , Rodriguez E , et al. Carbon-based sorbents impregnated with iron oxides for removing mercury in energy generation processes [J]. Energy, 2018, 159(9):648-655.
14. He S, Zhou JS, Zhu Y, Luo ZY, Ni M, Cen KF. Mercury oxidation over a vanadia-based selective catalytic reduction catalyst [J]. Energy Fuels. 2008, 23,253–259.
15. Granite E, Pennline H, Hargis R. Novel sorbents for mercury removal from flue gas [J]. Ind Eng Chem Res 2000, 39, 1020-1029.